Available online at www.sciencedirect.com
ScienceDirect
Bioorganic & Medicinal Chemistry Letters 18 (2008) 1910–1915
Bioorganic & Medicinal Chemistry Letters

Identification and optimization of a novel series of [2.2.1]-oxabicyclo imide-based androgen receptor antagonists

Mark E. Salvati,[a,*] Aaron Balog,[a] Weifang Shan,[a] Richard Rampulla,[a] Soren Giese,[a] Tom Mitt,[a] Joseph A. Furch,[a] Gregory D. Vite,[a] Ricardo M. Attar,[a] Maria Jure-Kunkel,[b] Jieping Geng,[b] Cheryl A. Rizzo,[b] Marco M. Gottardis,[b] Stanley R. Krystek,[c] Jack Gougoutas,[c] Michael A. Galella,[c] Mary Obermeier,[d] Aberra Fura[d] and Gamini Chandrasena[d]

[a]*Department of Oncology Chemistry, Bristol-Myers Squibb Pharmaceutical Research and Development, PO Box 4000, Princeton, NJ 08543-4000, USA*
[b]*Department of Discovery Biology, Bristol-Myers Squibb Pharmaceutical Research and Development, PO Box 4000, Princeton, NJ 08543-4000, USA*
[c]*Department of Macromolecular Structure, Bristol-Myers Squibb Pharmaceutical Research and Development, PO Box 4000, Princeton, NJ 08543-4000, USA*
[d]*Pharmaceutical Candidate Optimization Department, Bristol-Myers Squibb Pharmaceutical Research and Development, PO Box 4000, Princeton, NJ 08543-4000, USA*

Received 25 December 2007; accepted 1 February 2008
Available online 8 February 2008

Abstract—A novel series of [2.2.1]-oxabicyclo imide-based compounds were identified as potent antagonists of the androgen receptor. Molecular modeling and iterative drug design were applied to optimize this series. The lead compound [3*aS*-(3*a*α,4β,5β,7β,7*a*α)]-4-(octahydro-5-hydroxy-4,7-dimethyl-1,3-dioxo-4,7-epoxy-2*H*-isoindol-2-yl)-2-iodobenzonitrile was shown to have potent in vivo efficacy after oral dosing in the CWR22 human prostate tumor xenograph model.
Published by Elsevier Ltd.

Carcinoma of the prostate (CaP) is the 2nd leading cause of cancer related death in men in the United States.[1] The androgen receptor (AR) is a ligand binding transcription factor in the nuclear hormone receptor super family and is a key molecular target in the etiology and progression of prostate cancer. Androgen ablation via surgical castration or by chemical castration with a luteinizing hormone releasing hormone agonist, in combination with an anti-androgen,[2] is currently the treatment of choice for advanced CaP. Although this therapy initially shows an 80–90% response rate,[3] approximately 50% of patients progress to fatal androgen independent CaP (AI-CaP) after about 18 months of treatment.[4] Recent data have shown that cytotoxic agents such as Docetaxel[5] can be effective in the treatment of AI-CaP, however the survival benefit is minimal. Recent advances in the field have shown that reactivation of the AR signaling pathway is the root cause for the development of AI-CaP.[6] The identification of the role of the AR in AI-CaP suggests that new agents which act at the level of the AR may be effective in the treatment of this disease. For this reason, we are interested in identifying novel small molecule antagonists of the AR that are more effective than the current AR antagonists at targeting the AR in AI-CaP.

Previous work from our laboratories has described a series of bicyclic imide[7] and hydantoin-based[8] AR antagonists (**1**, **2** & **3**, Table 1). As found with the clinically used anti-androgens bicalutamide[3] (**4**) and hydroxyflutamide[3] (**5**), our series of AR antagonists demonstrated potent binding (K_i) to, and functional antagonism (IC_{50}) of the wild type (WT) AR as found in the MDA-453 cell line.[9] Subsequent efforts led to

Keywords: Androgen receptor; Prostate cancer; AR antagonist; CWR22R; [2.2.1]-Oxabicyclo.
* Corresponding author. Tel.: +1 609 818 5259; fax: +1 609 818 5880; e-mail: mark.salvati@bms.co

0960-894X/$ - see front matter Published by Elsevier Ltd.
doi:10.1016/j.bmcl.2008.02.006

Table 1. Initial AR antagonist leads

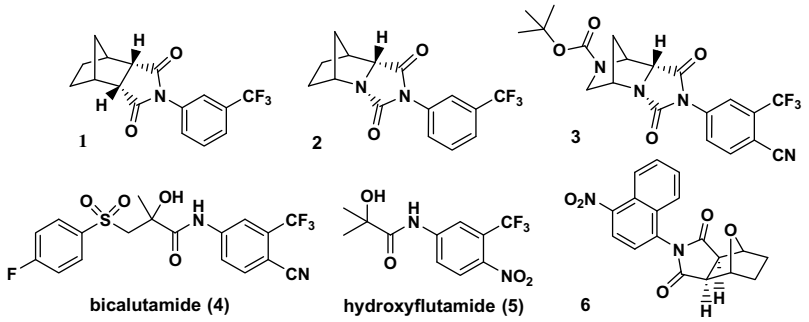

Compound #	MDA-453 K_i[a] (nM)	MDA-453 IC_{50}[b] (nM)
1	360	152
2	21	130
3	40	774
4	64	173
5	43	26
6	3.0	>5000

[a] Binding (K_i) determined through direct displacement with [^{3}H]-DHT in the MDA-453 cell line.[9]
[b] Functional antagonist activity (IC_{50}) determined through a transiently transfected reporter assay system utilizing the secreted alkaline phosphatase reporter gene driven by the AR-dependent, PSA promoter.[9]

the discovery of a new series of [2.2.1]-oxabicyclo imide-based analogs (**6**)[9,10] which demonstrated potent binding to, but weak antagonism of the WT AR. Mouse oral PK studies of key analogs from our imide, hydantoin and oxabicyclo series of AR antagonists, as well as bicalutamide (Table 2), revealed that of our three series, the oxabicyclo series possessed the most optimal oral PK profile. As our goal was to identify a new orally active anti-androgen for the treatment of CaP, we focused on improving the in vitro profile of our new [2.2.1]-oxabicyclo imide-based AR antagonists.

Table 2. Mouse oral PK profiles[11]

Compound #	Dose (mmol/kg)	C_{max} (μM)	T_{max} (h)	AUC (0–6 h) μM h
Bicalutamide (**4**)	0.1	110	0.5	768
1	0.1	0.023	0.5	0.056
2	0.1	1.74	0.5	11.4
6	0.1	100	0.5	11.4

For our first approach to improve upon the lead compound **6**, we explored replacement of the 4-nitronaphthyl group with a series of substituted aniline and naphthyl groups which had previously been shown to improve antagonist activity in our earlier series.[7,8,10,12] As shown in Table 3, all attempts to replace the 4-nitronaphthyl group led to a dramatic drop in binding to the AR (K_i), but improved overall antagonist activity (IC_{50}).

To aid us in our efforts to improve the potency of our [2.2.1]-oxabicyclo imide series, we turned to a modeling

Table 3. SAR around aniline and naphthyl portion[a]

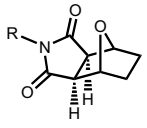

R	K_i (nm)	MDA 453 IC_{50} (nm)	Compound #	R	K_i (nM)	MDA 453 IC_{50}
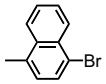	53.0	670	**11**	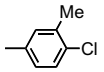	77.0	500
	221	350	**12**	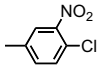	692	1150
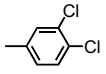	377	480	**13**	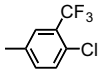	1110	3310
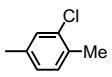	486	2290	**14**	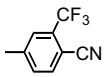	1170	2860

[a] Synthesis previously described.[10,12] See Scheme 1.

approach. Previous efforts from this lab have led to the first crystal structures of the AR with DHT as well as small molecule analogs from our earlier bicyclic imide series.[13,7] Using our available structural information, we constructed a model of compound **6** bound into the AR ligand binding domain (LBD).[14] Utilizing the minimized model shown in Figure 1, we explored potential sites where we could engineer interactions between compound **6** and the AR LBD protein backbone. As seen in Figure 1, we noted that adjacent to the C-4 and C-7 positions of the oxabicyclo ring system are two methionine residues (M780 and M895). M780 is located on the linker region between helix 6 and 7, on one side of the ligand binding pocket, while M895 resides on the hinge region of helix 12, on the opposite side of the ligand binding pocket. Extending a methyl group from the C-4 and C-7 position of the oxabicyclo core should result in positive lipophilic interactions with each of the methionine residues, generating improved binding of the ligand to the LBD. The crystal structure of AR

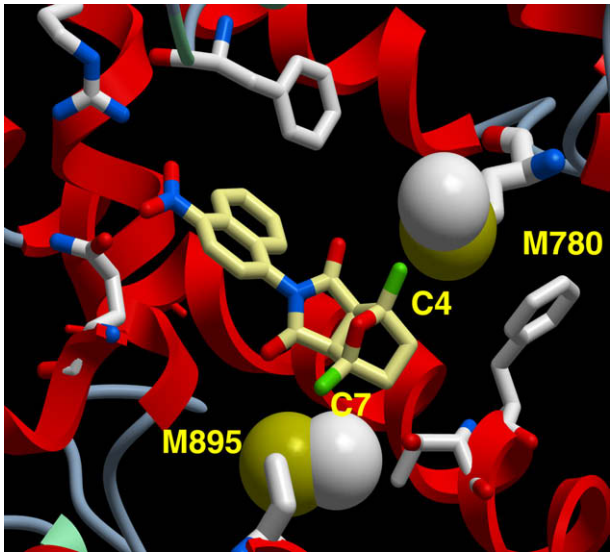

Figure 1. (A) Docking of a probe compound into the AR LBD. View of AR LBD binding site with a portion of the backbone ribbon (red) removed for clarity. Key side chains are displayed and colored by atom type (C white, N blue, O red). Residues M780 and M895 are in gold CPK rendering. Probe compound is shown in stick form colored by atom type (C yellow, N blue, O red) with the C-4 and C-7 methyl groups in green.

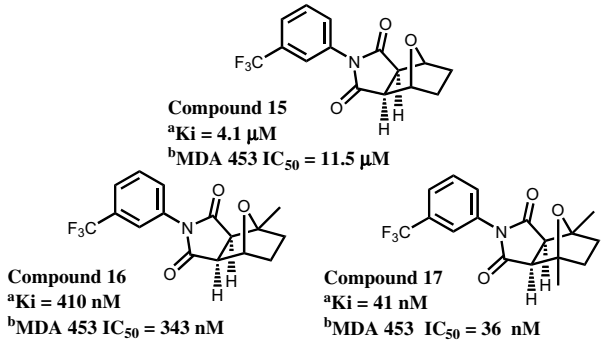

Figure 2. Effects of methyl groups at C-4 and C7 positions.

Table 4. SAR around aniline portion for 4,7-dimethyl analogs[a]

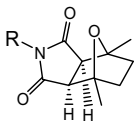

Compound #	R	K_i[a] (nM)	MDA 453[b] IC_{50} (nM)
18	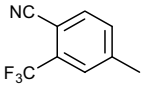	17	7.0
19	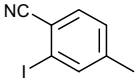	1.0	7.0
20	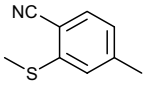	3.0	19
21	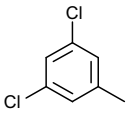	3.0	16
22	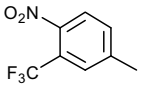	17	11
23	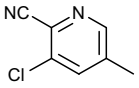	4.0	38
24	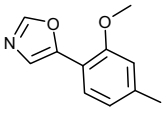	12	20
25	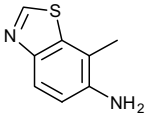	17	120
26	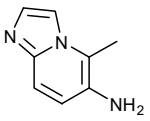	27	70
27	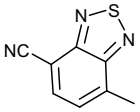	3.0	16
28	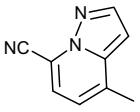	18	88
29	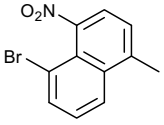	17	40

[a] Synthesis previously described.[12] See Scheme 1.

with DHT shows a similar interaction between M780 and the C15-C16 atoms of DHT.[13] Additional AR co-crystal structures demonstrate interactions between M895 and residues from several non-steroidal AR agonists.[15]

To validate this model, we designed a series of [2.2.1]-oxabicyclo imide analogs having a methyl at the C-4 or both the C-4 and C-7 positions of the molecule.[10,12] Figure 2 shows the results of one set of analogs synthesized. Compound **15** demonstrates weak binding to and antagonism of the AR. Addition of a C-4 methyl group (compound **16**), demonstrates a 10-fold improvement in binding and antagonist activity. The opposite antipode of compound **16** showed a similar increase in binding to the AR (data not shown). Addition of a second methyl at the C-7 position yields compound **17**, which again results in a 10 fold increase in both binding and potency as compared to the mono-methyl analog **16**. To expand on this observation, we once again explored an array of substitutions at the aniline portion of the molecule. As seen in Table 4, addition of a methyl group at the C-4 and C-7 position of the [2.2.1]-oxabicyclo imide core consistently resulted in improved binding to and antagonism of the AR though a wide variety of aniline replacements. Through this exercise, we were able to identify compound **19** as the most potent analog in our series. Compound **19** demonstrates a 64-fold improvement in binding affinity and a 25-fold improvement in antagonist activity as compared to bicalutamide (**4**). Despite the potent activity of compound **19**, this compound was found to be rapidly metabolized by liver microsomes (human liver microsome rate: 0.8 nmol/min/mg protein),[16] and thus was not suitable for progression as an oral agent.

Past work in our group and literature reports[10,12,17] had shown that functionalization at the C-5 position of the oxo-bicyclo ring system resulted in improved metabolic stability. Based on this observation, we synthesized the C-5 hydroxyl analog of compound **19**. Scheme 1 shows the general pathway used to make the two enantiomers of the C-5 hydroxylated analog of compound **19**, details of which have previously been published.[12] The synthesis begins with commercially available 4-nitroaniline which is treated with I_2 in the presence of $AgSO_4$ to yield

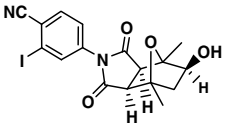

Compound 34a:
[a,c]Ki = 7.18 ± 1.21 nM
[b]MDA 453 IC_{50} =10 nM
Human liver microsome rate:
0.001 nmol/min/mg protein

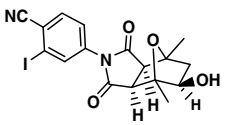

Compound 34b:
[a,c]Ki = 2.41 ± 0.18 nM
[b]MDA 453 IC_{50} = 19 nM
Human liver microsome rate:
0.04 nmol/min/mg protein

[c]Value calculated as average of 5 test occasions

Figure 3. Lead compounds **34a** and **34b**.

2-iodo-4-nitroaniline. 2-Iodo-4-nitroaniline was treated with $NaNO_2$ to form the diazonium salt, which was then treated with a mixture of CuCN and KCN to yield 2-iodo-4-nitrobenzonitrile. Reduction of the nitro group was achieved with iron powder to give 4-amino-2-iodobenzonitrile (**30**). 4-Amino-2-iodobenzonitrile and furan-2,5-dione (**31**) were heated together in the presence of acetic acid to yield 4-(2,5-dioxo-2,5-dihydro-1*H*-pyrrol-1-yl)-2-iodobenzonitrile (**32**), which was carried forward in a Diels–Alder reaction with 2,5-dimethylfuran to yield intermediate **33**. Hydroboration of intermediate **33** is achieved through treatment with borane-dimethylsulfide to yield the racemic mixture of compounds **34a** and **34b**, which were separated by chiral HPLC using standard conditions. The crystal structure of compound **34a** was determined, establishing the absolute stereochemistry of both enantiomers.[18]

As seen in Figure 3, enantiomers **34a** and **34b**, demonstrated high metabolic stability in liver microsomes and potent binding to, and antagonism of, the AR. Enantiomer **34b** demonstrated an 3-fold increase in binding relative to **34a**, even though this compound showed a slight decrease in antagonist activity. With this data, we returned to our original model to try to better understand the difference in binding found between the two enantiomers. Figure 4A and B shows the binding models for both enantiomers **34a** and **34b** in the AR LBD structure. Interestingly, the models suggest that for both enantiomers **34a** and **34b** a H-bond can exist between the bridgehead oxygen as well as the C-5 hydro-

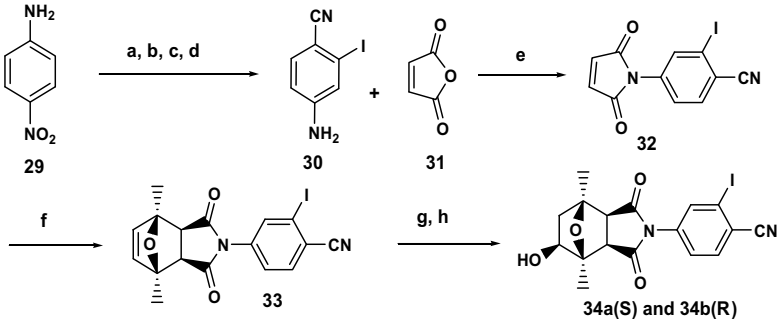

Scheme 1. Synthesis of C-5 hydroxy compounds **34a** and **34b**. Reagents and conditions: (a) I_2, $AgSO_4$, EtOH, 22 °C (95%); (b) $NaNO_2$, HCl, H_2O, 0 °C, then $NaBF_4$, 0 °C; (c) CuCN (0.1 equiv), KCN (1.0 equiv), H_2O, 22 °C (44% over b and c); (d) iron powder (325 mesh), NH_4Cl (aq), THF, EtOH, 60 °C (97%); (e) AcOH, 110 °C (90%); (f) neat 2,5-dimethylfuran, 60 °C (94%); (g) borane-dimethylsulfide, 0–25 °C, then Na_2HPO_4/KH_2PO_4 (pH 7), H_2O_2, 0 °C (25%); (h) chiral HPLC.

xyl group and N-705 of helix 3, in the AR LBD binding pocket. In previous AR co-crystal structures, the N705 residue has been shown to make critical hydrogen bond interactions with the C-17 hydroxyl group of DHT[13] as well as key hydroxyl residues of other non-steroidal AR agonist ligands.[15] In the case of enantiomer **34b**, an additional H-bond may occur from the C-5 hydroxyl group to T877 of the AR LBD, which completely recapitulates the bifurcated hydrogen bond network seen with the C-17 hydroxyl of DHT to T877 of the AR LBD in the co-crystal structure.[13] Thus, the model appears to predict the observed binding data and suggests that compound **34b** should have improved binding relative to compound **34a**, due to the additional formation of an H-bond to T-877. As is often noted for ligands of nuclear hormone receptors, the binding affinities of compounds **34a** and **34b** do not correlate with their functional antagonist activities.

Due to the improved metabolic stability[16] and suitable antagonist activity found with compound **34a**, we advanced this compound forward into efficacy studies in the CW22R human tumor xenograft model.[19] Compound

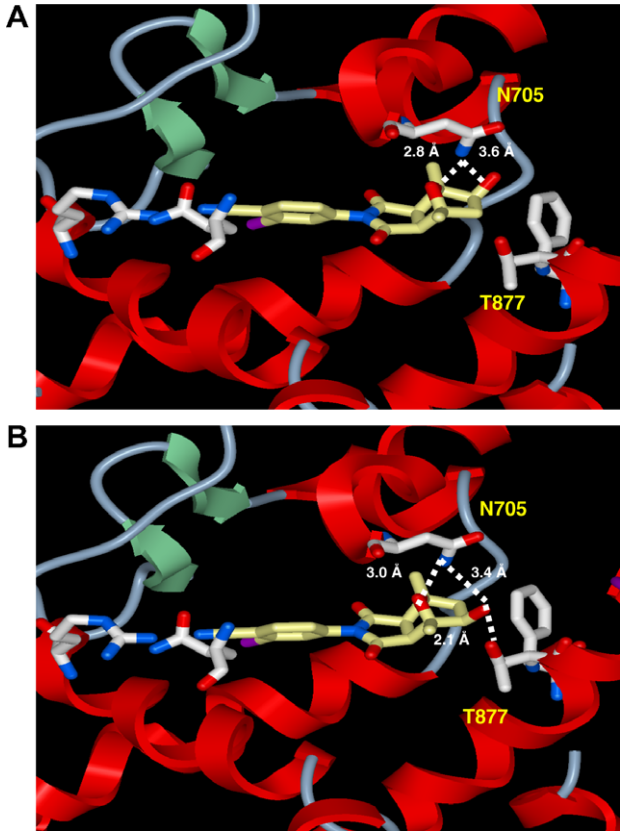

Figure 4. (A) Docking of compound **34a** into the AR LBD. (B) Docking of compound **34b** into the AR LBD. View of AR LBD binding site with a portion of the backbone ribbon (red) removed for clarity. Key side chains are displayed and colored by atom type (C white, N blue, O red). Dotted lines signify potential hydrogen bonds from key amino acid residues (N705 and T877) to specific atoms on ligands with the distance of each potential hydrogen bond listed in angstroms. Compound **34a** and **34b** are shown in stick form colored by atom type (C yellow, N blue, O red).

Table 5. CWR22R xenograft study: mice were dosed orally in a vehicle of PEG-400/Tween 80 (80:20) for 62 consecutive days with compound **34a** or bicalutamide (**4**)

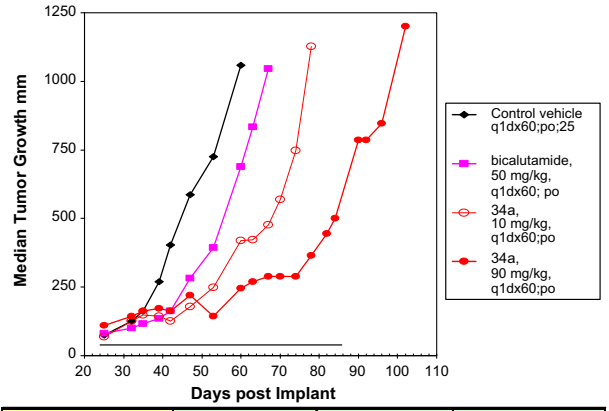

Drug	34a	34a	bicalutamide (4)
Dose (mpk)	10	90	50
Mean exposure @ 1 and 24 h (μM)	26, 8	55.5, 23.6	48.5, 86.0
Stdev (μM)	3, 1.7	4.6, 15.6	19.4, 11.0

Plasma samples were taken 1 and 24 h post-dose on day 60 and drug concentrations were measured.[21] Tumor volumes were measured twice weekly.[21]

34a was tested along side bicalutamide (**4**) in this model, with daily oral dosing. As can been seen in Table 5, compound **34a** demonstrated superior efficacy in this model despite achieving significantly lower plasma levels than that of bicalutamide. It should be noted that the dose of bicalutamide used in these studies generates plasma levels consistent with levels clinically found in humans.[20]

In summary, we have identified a novel series of [2.2.1]-oxabicycloimide-based AR antagonists. Through molecular modeling approaches and an iterative drug design process we identified several unique contact points in the AR LBD binding pocket which we were able to exploit to increase the affinity of our early [2.2.1]-oxabicyclo imide-based leads. Ultimately, we were able to identify the highly potent compounds **34a** and **34b**. Compound **34a** demonstrated significantly improved efficacy relative to the clinically used anti-androgen bicalutamide (**4**) in the CWR22R human prostate xenograft model. This work serves to demonstrate pre-clinical proof of concept that novel AR antagonists can be developed that may demonstrate improved efficacy for the treatment of advanced CaP. The unique interactions identified through our application of modeling have since been exploited in the design of additional novel AR antagonists for the treatment of advanced CaP, the subject of which will be described elsewhere.

References and notes

1. Jemal, A.; Thomas, H.; Murray, T.; Thun, M. *CA Cancer J. Clin.* **2002**, *52*, 23.
2. (a) Gao, K. L. *Drugs* **1991**, *43*, 254; (b) Motta, M.; Serio, M. *Hormonal Therapy of Prostatic Diseases: Basic and Clinical Aspects*; Medicom Europe: Amsterdam, 1998; (c)

Crawford, E. D.; DeAntonio, E. P.; Labrie, F.; Schroder, F. H.; Geller, J. *J. Clin. Endocrinol. Metab.* **1995**, *80*, 1062.
3. (a) Blackledge, G. *Cancer* **1993**, 3830; (b) Maucher, A.; von Angerer, E. *J. Cancer Res. Clin. Oncol.* **1993**, *119*, 669; (c) Sufrin, G.; Coffey, D. S. *Invest. Urol.* **1976**, *13*, 429; (d) Narayana, A. S.; Loening, S. A.; Culp, D. A. *Br. J. Urol.* **1981**, *53*, 152.
4. Huggins, C.; Stevens, R.; Hodges, C. V. *Arch. Surg.* **1947**, *43*, 209; Westin, P.; Stattin, P.; Damber, J.-E.; Bergh, A. *Am. J. Pathol.* **1995**, *146*, 1368.
5. Krainer, M.; Tomek, S.; Elandt, K.; Horak, P.; Albrecht, W.; Eisenmenger, M.; Hölt, W.; Schramek, P.; Stackl, W.; Zielinski, C.; Reibenwein, J. *J. Urol.* **2007**, *177*, 2145; González-Martin, A.; Fernández, E.; Vaz, MA.; Burgos, J.; López García, A.; Rodríguez Patrón, R.; Guillén, C.; Mayayo, T.; Allona, A.; Arias, F.; Moyano, A. *Clin. Transl. Oncol.* **2007**, *9*, 323.
6. Scher, H.; Sawyers, C. *J. Clin. Oncol.* **2005**, *23*, 8253; Chen, C. D.; Welsbie, D. S.; Tran, C.; Baek, S.-H.; Chen, R.; Vessella, R.; Rosenfeld, M. G.; Sawyers, C. L. *Nat. Med.* **2004**, *10*, 33; Richter, E.; Srivastava, S.; Dobi, A. *Prostate Cancer Prostatic Dis.* **2007**, *10*, 114; Burd, C. J.; Morey, L. M.; Knudsen, K. E. *Endocr. Relat. Cancer* **2006**, *13*, 979; Hendriksen, P. J. M.; Dits, N. F. J.; Kokame, K.; Veldhoven, A.; van Weerden, W. M.; Bangma, C. H.; Trapman, J.; Jenster, G. *Cancer Res.* **2006**, *66*, 5012.
7. Salvati, M.; Balog, A.; Wei, D.; Pickering, D.; Attar, R.; Geng, J.; Rizzo, C.; Hunt, J.; Weinmann, R.; Martinez, R. *Bioorg. Med. Chem. Lett.* **2005**, *15*, 289.
8. (a) Balog, A.; Shan, W.; Salvati, M.; Mathur, A.; Leith, L.; Wei, D.; Attar, R.; Geng, J.; Rizzo, C.; Wang, C.; Krystek, S.; Tokarski, J.; Hunt, J.; Weinmann, R. *Bioorg. Med. Chem. Lett.* **2004**, *14*, 6107; (b) Salvati, M.; Balog, A.; Shan, W.; Wei, D.; Pickering, D.; Attar, R.; Geng, J.; Rizzo, C.; Gottardis, M.; Weinmann, R.; Krystek, S.; Sack, J.; An, Y.; Kish, K. Design, Structural Analysis and Biological Profile of a Novel Series of AR Antagonists, Poster Presentation, American Association of Cancer Research, 95th Annual Meeting, 2004.
9. Salvati, M. E.; Balog, A.; Pickering, D. A.; Giese, S.; Fura, A.; Li, W.; Patel, R.; Hanson, R. L.; Mitt, T.; Roberge, J.; Corte, J. R.; Spergel, S. H.; Rampulla, R. A.; Misra, R.; Xiao, H.-Y. WO 2003062241.
10. Salvati, M.; Attar, A.; Balog, A.; Gottardis, M.; Krystek, S.; Rampulla, R.; Pickering, D.; Giese, G.; Shan, W.; Wei, D.; Zhu, H., Mathur, A., Geng, J. Rizzo, C.; Jure-Kunkel, M.; Dell, J.; Spires, T.; Kukral, Db. Oral Presentation, 227th ACS National Meeting and Exposition, Fall 2005.
11. The pharmacokinetics of test compounds were investigated in male Balb/C mice. Groups of three male mice (20 ± 2 g) received a single oral dose of test compound at 10 mg/kg in PEG 400/water (80:20, v/v). The animals were fasted overnight prior to dosing. After dosing, serial blood samples were collected, by retro-orbital bleeding, in microcentrifuge tubes at predose, 10, 30 min and 1, 2, 4, 6, 8, 10, and 24 h post-dose. Three blood samples were obtained from each mouse. Samples from three mice were obtained for each blood collection time point for a composite pharmacokinetic profile. The blood volume collected at each time point was 0.2 mL. Blood samples were immediately centrifuged at 4 °C and the separated serum was frozen on dry ice and stored at −20 °C until LC/MS/MS analysis under standard conditions.
12. Salvati, M.; Balog, A.; Pickering, D.; Giese, S.; Fura, A.; Wenying, L.; Patel, R.; Hanson, R.; Mitt, T.; Roberge, J.; Corte, J.; Spergel, S.; Rampulla, R; Misra, R.; Xiao, H.-Y. US-7,141,578 B2.
13. Sack, J. S.; Kish, K.; Wang, C.; Attar, M.; Kiefer, S. E.; Yongmi, W.; Ginger, Y.; Scheffler, J. E.; Salvati, M. E.; Krystek, S. R.; Weinmann, R.; Einspahr, H. M. *Proc. Natl. Acad. Sci.* **2001**, *98*, 4904.
14. (a) Molecular modeling was performed using ICM software (Molsoft LLC, San Diego, CA). The docking of the ligands into WT AR LBD was carried out using the ICM docking procedure which is a two step process. Initial docking of ligands were carried out using grid potential representation of the receptor and flexible ligand. Five grid potentials describe the shape, hydrophobicity, electrostatics, and hydrogen bonding potential of the receptor. The conformations from the grid were then optimized with a full atom representation of the receptor and flexible ligand, by an ICM stochastic global optimization algorithm as implemented in version 2.7 of the Molsoft ICM program (Refs. a and b). (a) Molsoft (1998) ICM 2.7 Program Manual (Molsoft, San Diego, CA); (b) Totrov, M.; Abagyan, R. *Proteins Suppl.* **1997**, *1*, 215.
15. Bohl, C. E.; Miller, D. D.; Chen, J.; Bell, C. E.; Dalton, J. T. *J. Biol. Chem.* **2005**, *280*, 37747; Bohl, C. E.; Wu, Z.; Miller, D. D.; Bell, C. E.; Dalton, J. T. *J. Biol. Chem.* **2007**, *282*, 13648; Cantin, L.; Faucher, F.; Couture, J.-F.; de Jésus-Tran, K. P.; Pierre, L.; Ciobanu, L. C.; Fréchette, Y.; Labrecque, R., Singh, S. M.; Labrie, F.; Breton, R. *J. Biol. Chem.* **2007** Manuscript M705524200.
16. In vitro metabolism was determined using pooled human liver microsomes. The liver microsomal incubation mixtures contain the substrate compound (10 μM in DMSO), microsomal protein (1 mg/mL), NADPH (1 mM), and phosphate buffer (56 mM, pH 7.4). The reaction, was conducted in triplicate, was initiated by the addition of NADPH followed by incubation at 37 °C for 120 min. Aliquots of samples (0.2 mL) were taken at various time points over 120 min, and the reaction was quenched by the addition of an equal volume of acetonitrile. Samples were analyzed by standard HPLC method by comparing the peak area ratio of the samples at each time point to the peak area ratios at 0 h. The rate of metabolism was determined from the amount of the parent compound consumed per min per mg of microsomal protein used in the assay.
17. Dockens, R. C.; Santone, K. S.; Mitroka, J. G.; Morrison, R. A.; Jemal, M.; Greene, D.; Barbhaiya, R. H. *Drug Met. Dis.* **2000**, *28*, 973.
18. Structure submitted into the Cambridge Structural Database, Reg# CCDC 664455.
19. Structural Database Chen, C.-T.; Gan, Y.; Au, J.; Wientjes, M. *Cancer Res.* **1998**, *59*, 2777.
20. Cockshott, I. D.; Oliver, S. D.; Young, J. J.; Cooper, K. J.; Jones, D. C. *Biopharm. Drug Dis.* **1997**, *18*, 499; Blackledge, G. *Cancer Suppl.* **1993**, *72*, 3830.
21. Blood samples were collected, by retro-orbital bleeding, in microcentrifuge tubes at 1 and 24 h post-dose. Sample work-up and analysis were as described in Ref. 10. Details for the experimental procedure used for the CWR22 Human Prostate Xenograft study can be found in US-7,141,578 B2.